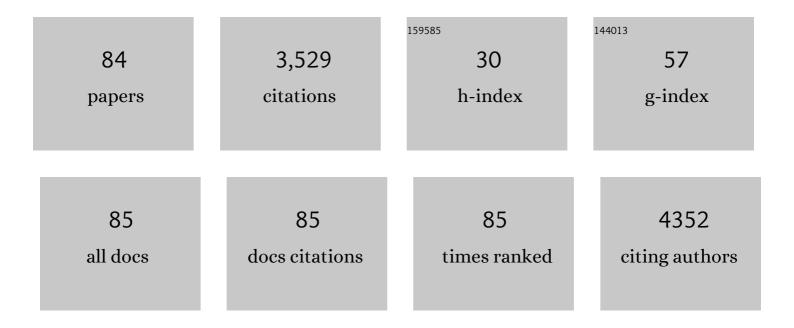
Zhifeng Shao

List of Publications by Year in descending order

Source: https://exaly.com/author-pdf/3423822/publications.pdf Version: 2024-02-01



#	Article	IF	CITATIONS
1	Epithelial Cells in 2D and 3D Cultures Exhibit Large Differences in Higher-order Genomic Interactions. Genomics, Proteomics and Bioinformatics, 2022, 20, 101-109.	6.9	4
2	Robust Acquisition of Spatial Transcriptional Programs in Tissues With Immunofluorescence-Guided Laser Capture Microdissection. Frontiers in Cell and Developmental Biology, 2022, 10, 853188.	3.7	3
3	Single-Molecule Micromanipulation and Super-Resolution Imaging Resolve Nanodomains Underlying Chromatin Folding in Mitotic Chromosomes. ACS Nano, 2022, 16, 8030-8039.	14.6	7
4	Threeâ€Dimensional Quantitative Imaging of Native Microbiota Distribution in the Gut. Angewandte Chemie - International Edition, 2021, 60, 3055-3061.	13.8	31
5	Threeâ€Dimensional Quantitative Imaging of Native Microbiota Distribution in the Gut. Angewandte Chemie, 2021, 133, 3092-3098.	2.0	1
6	High-resolution single-cell 3D-models of chromatin ensembles during Drosophila embryogenesis. Nature Communications, 2021, 12, 205.	12.8	17
7	Ratiometric Raman nanotags enable intraoperative detection of metastatic sentinel lymph node. Biomaterials, 2021, 276, 121070.	11.4	12
8	Nanomechanical Induction of Autophagyâ€Related Fluorescence in Single Cells with Atomic Force Microscopy. Advanced Science, 2021, 8, e2102989.	11.2	10
9	Monocytic THP-1 cells diverge significantly from their primary counterparts: a comparative examination of the chromosomal conformations and transcriptomes. Hereditas, 2021, 158, 43.	1.4	8
10	Controlling Water Flow through a Synthetic Nanopore with Permeable Cations. ACS Central Science, 2021, 7, 2092-2098.	11.3	8
11	Evidence for heightened genetic instability in precancerous spasmolytic polypeptide expressing gastric glands. Journal of Medical Genetics, 2020, 57, 385-388.	3.2	6
12	Q-Nuc: a bioinformatics pipeline for the quantitative analysis of nucleosomal profiles. Interdisciplinary Sciences, Computational Life Sciences, 2020, 12, 69-81.	3.6	6
13	Significant improvement in data quality with simplified SCRB-seq. Acta Biochimica Et Biophysica Sinica, 2020, 52, 457-459.	2.0	5
14	Ultrasensitive liposome-based assay for the quantification of fundamental ion channel properties. Analytica Chimica Acta, 2020, 1112, 8-15.	5.4	7
15	CHROMATIX: computing the functional landscape of many-body chromatin interactions in transcriptionally active loci from deconvolved single cells. Genome Biology, 2020, 21, 13.	8.8	22
16	Massive reorganization of the genome during primary monocyte differentiation into macrophage. Acta Biochimica Et Biophysica Sinica, 2020, 52, 546-553.	2.0	4
17	Wdr47 Controls Neuronal Polarization through the Camsap Family Microtubule Minus-End-Binding Proteins. Cell Reports, 2020, 31, 107526.	6.4	21
18	Atomic force microscopy-based single-molecule force spectroscopy detects DNA base mismatches. Nanoscale, 2019, 11, 17206-17210.	5.6	13

#	Article	IF	CITATIONS
19	Selective translational usage of TSS and core promoters revealed by translatome sequencing. BMC Genomics, 2019, 20, 282.	2.8	10
20	3D Segmentation of Mice Gland Based on Ensemble Learning. , 2019, , .		0
21	Sub-kb Hi-C in D. melanogaster reveals conserved characteristics of TADs between insect and mammalian cells. Nature Communications, 2018, 9, 188.	12.8	126
22	Super-resolution Imaging of Individual Human Subchromosomal Regions <i>in Situ</i> Reveals Nanoscopic Building Blocks of Higher-Order Structure. ACS Nano, 2018, 12, 4909-4918.	14.6	41
23	abLIM1 constructs non-erythroid cortical actin networks to prevent mechanical tension-induced blebbing. Cell Discovery, 2018, 4, 42.	6.7	10
24	Compressive Force Spectroscopy: From Living Cells to Single Proteins. International Journal of Molecular Sciences, 2018, 19, 960.	4.1	5
25	Characterization of DNA Methylation Associated Gene Regulatory Networks During Stomach Cancer Progression. Frontiers in Genetics, 2018, 9, 711.	2.3	8
26	Improved clearing of lipid droplet-rich tissues for three-dimensional structural elucidation. Acta Biochimica Et Biophysica Sinica, 2017, 49, 465-467.	2.0	9
27	Enforced Tubular Assembly of Electronically Different Hexakis(<i>m</i> -Phenylene Ethynylene) Macrocycles: Persistent Columnar Stacking Driven by Multiple Hydrogen-Bonding Interactions. Journal of the American Chemical Society, 2017, 139, 15950-15957.	13.7	39
28	Toward the development of magnetic tweezers for high-throughput measurement of protein–protein interactions. Acta Biochimica Et Biophysica Sinica, 2017, 49, 468-470.	2.0	0
29	Chitosan-based core-shell nanomaterials for pH-triggered release of anticancer drug and near-infrared bioimaging. Carbohydrate Polymers, 2017, 157, 325-334.	10.2	58
30	Identification of Biomarkers for Predicting Lymph Node Metastasis of Stomach Cancer Using Clinical DNA Methylation Data. Disease Markers, 2017, 2017, 1-7.	1.3	31
31	MALAT1 long ncRNA promotes gastric cancer metastasis by suppressing <i>PCDH10</i> . Oncotarget, 2016, 7, 12693-12703.	1.8	97
32	Ultra-deep sequencing of ribosome-associated poly-adenylated RNA in early <i>Drosophila</i> embryos reveals hundreds of conserved translated sORFs. DNA Research, 2016, 23, 571-580.	3.4	14
33	Epigenetic Profiling of H3K4Me3 Reveals Herbal Medicine Jinfukang-Induced Epigenetic Alteration Is Involved in Anti-Lung Cancer Activity. Evidence-based Complementary and Alternative Medicine, 2016, 2016, 1-13.	1.2	16
34	Single molecule atomic force microscopy of aerolysin pore complexes reveals unexpected starâ€shaped topography. Journal of Molecular Recognition, 2016, 29, 174-181.	2.1	7
35	Complex clonal mosaicism within microdissected intestinal metaplastic glands without concurrent gastric cancer. Journal of Medical Genetics, 2016, 53, 643-646.	3.2	6
36	Synthesis and micellization of redox-responsive dynamic covalent multi-block copolymers. Polymer Chemistry, 2016, 7, 3145-3155.	3.9	16

#	Article	IF	CITATIONS
37	Activation of AIFM2 enhances apoptosis of human lung cancer cells undergoing toxicological stress. Toxicology Letters, 2016, 258, 227-236.	0.8	34
38	Nanoscopic characterization of the water vapor-salt interfacial layer reveals a unique biphasic adsorption process. Scientific Reports, 2016, 6, 31688.	3.3	3
39	Integrative epigenomic analysis reveals unique epigenetic signatures involved in unipotency of mouse female germline stem cells. Genome Biology, 2016, 17, 162.	8.8	61
40	Development of a low-noise cryogenic atomic force microscope for high resolution imaging of large biological complexes. Acta Biochimica Et Biophysica Sinica, 2016, 48, 859-861.	2.0	1
41	Reductive triblock copolymer micelles with a dynamic covalent linkage deliver antimiR-21 for gastric cancer therapy. Polymer Chemistry, 2016, 7, 4352-4366.	3.9	9
42	The non-coding RNA composition of the mitotic chromosome by 5′-tag sequencing. Nucleic Acids Research, 2016, 44, 4934-4946.	14.5	16
43	Persistent Organic Nanopores Amenable to Structural and Functional Tuning. Journal of the American Chemical Society, 2016, 138, 2749-2754.	13.7	77
44	Large scale gene regulatory network inference with a multi-level strategy. Molecular BioSystems, 2016, 12, 588-597.	2.9	26
45	Identification of Serum Biomarkers for Gastric Cancer Diagnosis Using a Human Proteome Microarray. Molecular and Cellular Proteomics, 2016, 15, 614-623.	3.8	82
46	<i>Helicobacter pylori</i> CagA induces tumor suppressor gene hypermethylation by upregulating DNMT1 via AKT-NFή pathway in gastric cancer development. Oncotarget, 2016, 7, 9788-9800.	1.8	53
47	Fast immuno-labeling by electrophoretically driven infiltration for intact tissue imaging. Scientific Reports, 2015, 5, 10640.	3.3	40
48	Genome-wide profiling of polyadenylation sites reveals a link between selective polyadenylation and cancer metastasis. Human Molecular Genetics, 2015, 24, 3410-3417.	2.9	41
49	Redox-responsive micelles self-assembled from dynamic covalent block copolymers for intracellular drug delivery. Acta Biomaterialia, 2015, 17, 193-200.	8.3	74
50	Spatially defined microsatellite analysis reveals extensive genetic mosaicism and clonal complexity in intestinal metaplastic glands. International Journal of Cancer, 2015, 136, 2973-2979.	5.1	2
51	Developing the IVIG biomimetic, Hexa-Fc, for drug and vaccine applications. Scientific Reports, 2015, 5, 9526.	3.3	33
52	Chitosan oligosaccharide copolymer micelles with double disulphide linkage in the backbone associated by H-bonding duplexes for targeted intracellular drug delivery. Polymer Chemistry, 2015, 6, 1454-1464.	3.9	28
53	Illuminated up close: near-field optical microscopy of cell surfaces. Nanomedicine: Nanotechnology, Biology, and Medicine, 2015, 11, 119-125.	3.3	4
54	Single molecule compression reveals intra-protein forces drive cytotoxin pore formation. ELife, 2015, 4, e08421.	6.0	16

4

#	Article	IF	CITATIONS
55	Enhancing the effectiveness of fungicides by optimizing their combinations. , 2014, , .		0
56	Anomalous Surface Fatigue in a Nano‣ayered Material. Advanced Materials, 2014, 26, 6478-6482.	21.0	3
57	Mercury arc lamp based super-resolution imaging with conventional fluorescence microscopes. Micron, 2014, 59, 24-27.	2.2	4
58	Self-Assembling Organic Nanotubes with Precisely Defined, Sub-nanometer Pores: Formation and Mass Transport Characteristics. Accounts of Chemical Research, 2013, 46, 2856-2866.	15.6	186
59	Self-assembling subnanometer pores with unusual mass-transport properties. Nature Communications, 2012, 3, 949.	12.8	174
60	The human IgM pentamer is a mushroom-shaped molecule with a flexural bias. Proceedings of the National Academy of Sciences of the United States of America, 2009, 106, 14960-14965.	7.1	172
61	Highly Conducting Transmembrane Pores Formed by Aromatic Oligoamide Macrocycles. Journal of the American Chemical Society, 2008, 130, 15784-15785.	13.7	145
62	Vertical collapse of a cytolysin prepore moves its transmembrane β-hairpins to the membrane. EMBO Journal, 2004, 23, 3206-3215.	7.8	242
63	Characterization of AC mode scanning ion-conductance microscopy. Ultramicroscopy, 2001, 90, 13-19.	1.9	72
64	Near-field optical microscopy with a vibrating probe in aqueous solution. Applied Physics Letters, 2001, 78, 2076-2078.	3.3	23
65	Probing the structure of monomers and dimers of the bacterial virus phi29 hexamer RNA complex by chemical modification. Rna, 2000, 6, 1257-1266.	3.5	45
66	Optimum Window Size for Quantitating Trace Elements Using Linear Least Squares Fit With Eels. Microscopy and Microanalysis, 1999, 5, 938-939.	0.4	0
67	VacA fromHelicobacter pylori: a hexameric chloride channel. FEBS Letters, 1999, 450, 101-104.	2.8	125
68	Images of oligomeric Kvĺ²2, a modulatory subunit of potassium channels. FEBS Letters, 1999, 457, 107-111.	2.8	16
69	Calcium Quantitation with a Parallel Electron Energy Loss Spectroscopy/Cooled Charge-Coupled Device/200 keV System. Microscopy and Microanalysis, 1999, 5, 17-28.	0.4	4
70	Submolecular resolution of single macromolecules with atomic force microscopy. FEBS Letters, 1998, 430, 51-54.	2.8	82
71	Staphylococcal α-hemolysin can form hexamers in phospholipid bilayers 1 1Edited by W. Baumeister. Journal of Molecular Biology, 1998, 276, 325-330.	4.2	144
72	High resolution surface structure ofE. coliGroES oligomer by atomic force microscopy. FEBS Letters, 1996, 381, 161-164.	2.8	81

#	Article	IF	CITATIONS
73	Biological atomic force microscopy: what is achieved and what is needed. Advances in Physics, 1996, 45, 1-86.	14.4	331
74	A piezotube scanner for atomic force microscopy in solution. Review of Scientific Instruments, 1996, 67, 2654-2655.	1.3	7
75	The Effects of Non-Uniform Specimen Thickness on Thickness Determination and Elemental Quantitation with Electron Energy Loss Spectroscopy (EELS). Microscopy and Microanalysis, 1996, 2, 87-97.	0.4	1
76	Semiâ€automatic atomic force microscope for imaging in solution. Review of Scientific Instruments, 1995, 66, 5527-5531.	1.3	3
77	Progress in high resolution atomic force microscopy in biology. Quarterly Reviews of Biophysics, 1995, 28, 195-251.	5.7	155
78	Structure and stability of pertussis toxin studied by in situ atomic force microscopy. FEBS Letters, 1994, 338, 89-92.	2.8	63
79	An optical detection low temperature atomic force microscope at ambient pressure for biological research. Review of Scientific Instruments, 1993, 64, 1483-1488.	1.3	48
80	On the optical properties of an electrostatic retarding field lens. Journal of Vacuum Science and Technology A: Vacuum, Surfaces and Films, 1993, 11, 406-411.	2.1	2
81	SCANNING TUNNELING MICROSCOPY USING IONIC CONDUCTION FOR IMAGING NON-CONDUCTIVE SPECIMENS. Modern Physics Letters B, 1992, 06, 9-13.	1.9	6
82	Atomic force microscopy of DNA molecules. FEBS Letters, 1992, 301, 173-176.	2.8	98
83	Molecular resolution imaging of polyglucose by scanning tunneling microscopy. FEBS Letters, 1991, 279, 295-299.	2.8	9
84	Axial resolution of confocal microscopes with parallelâ€beam detection. Journal of Microscopy, 1991, 164, 13-19.	1.8	8